TIPS AND TRICKS FOR CHARACTERIZING SHAPE MEMORY ALLOY WIRE: PART 1—DIFFERENTIAL SCANNING CALORIMETRY AND BASIC PHENOMENA

by J.A. Shaw, C.B. Churchill, and M.A. Iadicola

Shape memory alloys (SMAs) are a fascinating group of metals that have two remarkable properties, the *shape memory effect* and *superelasticity*.[1,2] *Shape memory* refers to the recovery of shape (i.e., strain) after apparent "permanent" deformation (induced at relatively cold temperatures) by heating above a characteristic transformation temperature (often near room temperature [RT]). *Superelasticity* refers to the isothermal recovery of relatively large strains during a mechanical load–unload cycle that occurs at temperatures above a characteristic transformation temperature. A large number of SMAs have been discovered since the mid-1900s to late 1900s, and the list continues to grow.[3] Many of these alloys, while scientifically interesting, consist of precious metals or only exhibit useful properties as single crystals, which do not lend them to practical use in commercial applications. A few alloys, however, have emerged as commercially viable for novel devices. These include certain copper alloys (CuAlZn) and nickel–titanium–based alloys, such as near-equiatomic NiTi, known as Nitinol (first discovered in the early 1960s) and some ternary alloys such as NiTiCu and NiTiNb (see Fig. 1). To date, it is fair to say that NiTi-based SMAs have the best memory and superelasticity properties of all the known polycrystalline SMAs. The NiTi family of alloys can withstand large stresses and can recover strains near 8% for low cycle use or up to about 2.5% strain for high cycle use. This strain recovery capability can enable the design of novel devices in either a thermally active mode or an isothermal energy absorption mode. NiTi SMAs have other advantages in terms of corrosion resistance, fatigue resistance, and biocompatibility, thereby making them the preferred material system for most shape memory applications being considered today.

The materials science and mechanics literature regarding SMAs are vast, and we will not attempt a complete review here (see Otsuka and Ren[4] for a recent review). The field remains an active area of research, and the understanding of the mechanisms involved at all scales from the crystalline lattice to the macroscopic scale has progressed significantly, even during the past decade or so. Furthermore, advances in materials processing have resulted in production of Nitinol SMAs with good quality control, with reproducible properties, and in relatively large quantities. Nitinol wire, in particular, is being produced with excellent properties and is relatively inexpensive compared to most other forms. Applications of SMA wire are now being seriously considered even in cost-sensitive engineering sectors.[5] Consequently, our focus in this article is on the thermomechanical behavior of polycrystalline Nitinol wire under uniaxial tensile loading.

Shape memory alloys exhibit some rather surprising phenomena as well as extreme sensitivities to testing conditions, which can create pitfalls in material testing and interpretation for someone who is new to SMAs. As we like to say—it is not an amateur sport. Nevertheless, the need for high-quality data is increasingly common in industry, especially since small changes in chemistry or processing can result in both quantitative and qualitative differences in the material behavior, and new experimental alloys are continually being developed. Unfortunately, the testing of SMAs is not yet standardized (although there is work in this direction at ASTM), and unlike conventional alloys, material property tables either are not available or provide incomplete, or even incorrect, information for the user. This is, perhaps, not surprising since SMA behavior is nonlinear, hysteretic, and extremely temperature dependent, requiring more properties to be known than is usual for conventional alloys. Since each SMA is different, the user is often faced with testing SMAs in their own laboratory to obtain a satisfactory characterization of the material at hand. Even under simple tensile loading, performing meaningful experiments on SMA wire is not a trivial matter, and good practice is rarely explained sufficiently in the journal literature. We hope to fill that gap here by explaining some phenomena and describing techniques suitable for the engineer who may be relatively unfamiliar with testing SMA wire.

This is the first in a series of papers to introduce phenomena and subtleties that can lead to difficulties in testing SMA wire. Our aim is to introduce uninitiated engineers to the testing of SMAs and to highlight pitfalls in the interpretation of results. Accordingly, we will describe special experimental techniques that help to illuminate and quantify the macroscopic thermomechanical behavior. In this first paper (Part 1), we characterize transformation temperatures, specific heats, and latent heats by differential scanning calorimetry for two Nitinol wire alloys with different transformation temperatures. One exhibits shape memory above room temperature, and one exhibits superelasticity at room temperature. We give an overview of the unusual behavior of SMAs and its

Editor's Note: *This* ET *feature series is intended as an introduction to this exciting area of experimental mechanics. It aims to increase awareness of active materials and to promote their consistent characterization by disseminating best practices from leading researchers in the field. Each article in the series will address the characterization of one commercially significant active material. Series editors: Nilesh D. Mankame and Paul W. Alexander.*

J.A. Shaw (jashaw@umich.edu) is an associate professor and C.B. Churchill (churchc@umich.edu) is a PhD student affiliated with the Department of Aerospace Engineering, University of Michigan, Ann Arbor, MI. M.A. Iadicola is a metallurgist affiliated with the Materials Science and Engineering Laboratory, National Institute for Standards and Technology, Gaithersburg, MD.

doi: 10.1111/j.1747-1567.2008.00410.x
© 2008, Society for Experimental Mechanics

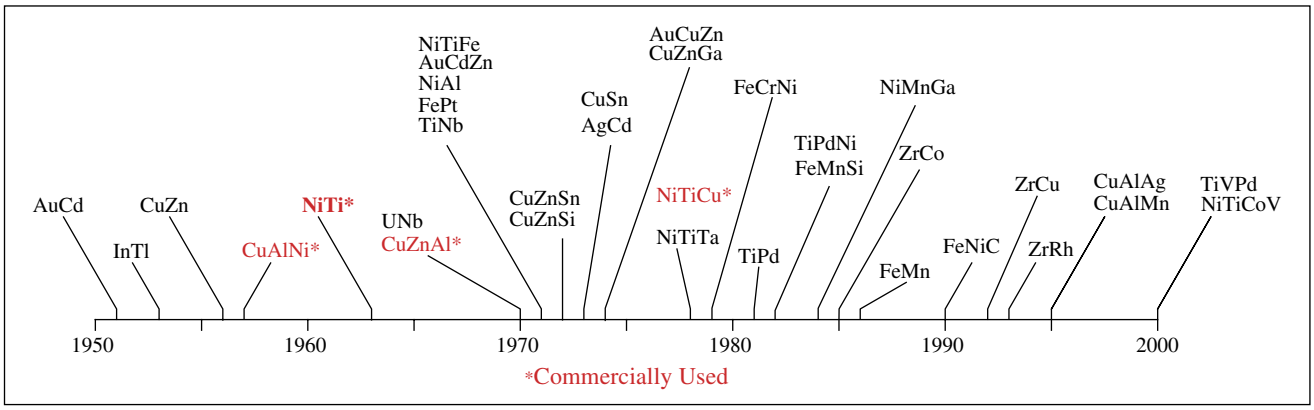

Fig. 1: History of the discovery of SMAs

origins, and demonstrate shape memory and superelasticity by special thermomechanical experiments. Future articles in this series will describe how mechanical responses are obtained to map material phases in stress–temperature space and will treat more advanced issues concerning material stability, loading rate effects, and cyclic shakedown, which require more specialized experimental techniques.

DIFFERENTIAL SCANNING CALORIMETRY

Both the shape memory effect and the superelasticity arise from *martensitic transformations* in the SMA material. Martensitic transformations are solid-to-solid phase transformations that occur without diffusion or plasticity, potentially making them reversible. They involve changes in the crystalline structure that can be induced by changes in either temperature or stress. The high-temperature, stress-free phase is called *austenite*, which has a high-symmetry crystal structure usually based on a cubic lattice. The low-temperature, stress-free phase is called *martensite*, which has a crystal structure with lower symmetry, such as tetragonal, rhombohedral, orthorhombic, monoclinic, or triclinic (see any standard introductory materials science text, such as Callister,[6] if these are unfamiliar), depending on the particular alloy. In Nitinol (near-equiatomic NiTi), the austenite has an ordered B2 crystal structure, which can be viewed as two interpenetrating simple cubic lattices of Ni and Ti, respectively. (It is often incorrectly called a body-centered cubic structure, which would only be accurate if the material were monoatomic.) The martensite has an ordered B19′ crystal structure, where B19 denotes an orthorhombic structure resulting from unequal normal strains relative to the <110> directions of the austenite structure, and the prime (′) indicates that it has additionally been distorted by a shear strain, resulting in monoclinic symmetry. Another intermediate phase that sometimes appears is called the *R* phase, which is a rhombohedral distortion of the B2 structure (see Fig. 2). (In the interest of simplicity, the figure ignores the complex stacking structures that actually occur in the superlattice. See Otsuka and Wayman[2] for details.) The gray planes shown in the figure's crystal structures indicate lattice correspondence planes between the standard unit cells shown.

The first step in characterizing an SMA material is to determine the characteristic transformation temperature. Actually, the material is hysteretic, and there are several transformation temperatures to speak of, including the austenite start temperature (A_s) and the austenite finish temperature (A_f) during heating and the martensite start temperature (M_s) and the martensite finish temperature (M_f) during cooling. Additionally, an intermediate phase (*R* phase) often appears during cooling, having its own start temperature (R_s) and finish temperature (R_f), before the transformation proceeds to martensite at lower temperatures. Under stress-free conditions, these are commonly measured by DSC thermograms either provided by the material supplier or obtained by the user. Alternate methods exist to measure transformation temperatures, such as electrical resistivity scanning, but while potentially convenient (in case a DSC machine is not available), they are more difficult to interpret and do not provide any information about latent heats of transformation or specific heats.

Two DSC Experiments

In this article, we focus on two different Nitinol alloys obtained from Memry Corp. (Bethel, CT), one that has a stress-free transformation above RT (termed "shape memory wire") and one that has a stress-free transformation below RT (termed "superelastic wire"). (Certain commercial equipment, instruments, or materials are identified in this article in order to specify the experimental procedure adequately. Such identification is neither intended to imply recommendation or endorsement nor intended to imply that the materials or equipment identified are necessarily the best available for the purpose.) It is well known that transformation temperatures of a Nitinol alloy can be tailored by the supplier anywhere from cryogenic temperatures to as high as about 100°C by small changes in chemistry, by aging heat

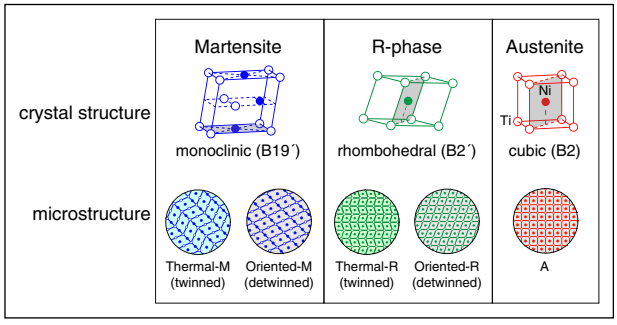

Fig. 2: Schematics of crystal structures and microstructures in Nitinol

treatments in the range 350–500°C, and by thermomechanical processing (cold work developed during wire drawing and/or cyclic loading performed by certain suppliers). The first-order effect on transformation temperatures is alloy chemistry. Just 1% excess Ni above stoichiometric NiTi (i.e., 50 at% Ni and Ti) can suppress transformation temperatures by over 100°C. While not measured directly, we suspect (based on typical supplier formulations) that our shape memory wire has a composition near 50.2 at% Ni, while the superelastic wire has a composition near 50.6 at% Ni (with the balance being Ti, except for trace amounts of other interstitial elements like C, N, and O). Our alloys were probably aged near 500°C for 10–15 min after cold working. These alloys were not subjected to any further thermomechanical cycling, so we term the as-received state as so-called "virgin Nitinol."

Differential scanning calorimetry thermograms for our two selected NiTi alloys are shown in Fig. 3. A small sample of material (typically 50–100 mg) was placed in a sample pan and then installed in a differential scanning calorimeter (Pyris 1 DSC; Perkin Elmer, Waltham, MA). The DSC is programmed by the user to scan the sample at a constant temperature rate while monitoring the heat flow rate, $\dot{Q}$, to the sample pan compared to another empty pan (hence the "differential" part of the name). The vertical scales in the figure have been converted to specific heat–like units, J/(gK), as described below. The upright peak and two upside-down peaks seen in each thermogram occur due to the respective endothermic (positive) and exothermic (negative) latent heats of transformation, respectively. The

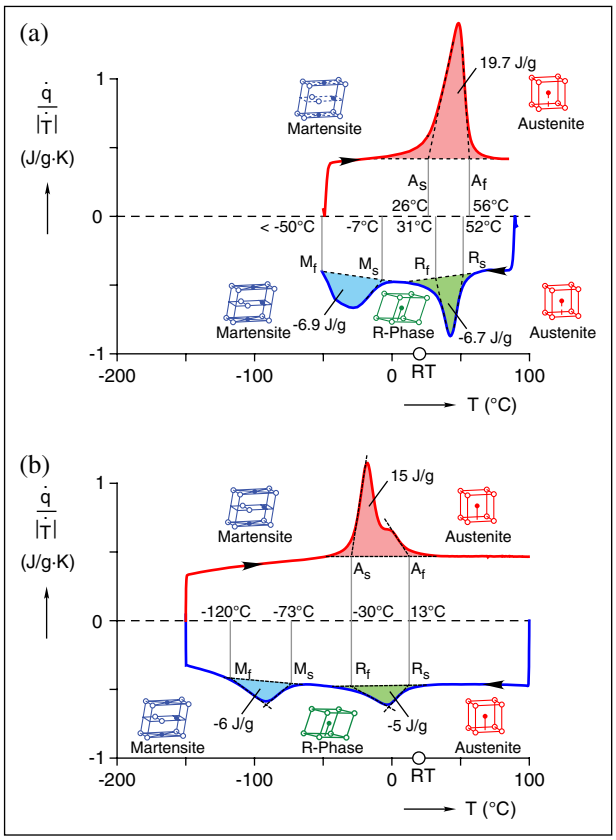

Fig. 3: Differential scanning calorimetry thermograms of two Nitinol alloys: (a) shape memory wire[7] and (b) superelastic wire[8]

peaks are bell shaped, so the start and finish temperatures of a transformation are typically extracted by a straight-line construction fitted to the steepest sides of the peak. The particular transformation temperature is read off the intersection of this line with a "baseline" that cuts off the peak. One can appreciate that this procedure has some uncertainty associated with it since it depends on the shape of the enthalpy peak and the baseline that is chosen.

The latent heat peaks separate temperature regimes where pure (or nearly so) solid-state phases exist. At sufficiently high temperature, the material is austenite, and at sufficiently low temperature, the material is thermal-martensite. At intermediate temperatures upon cooling, the material is thermal-*R* phase. As the temperature traverses a given latent heat peak, the material has a progressive mixture of the two phases from either side of the peak. Each peak represents "excess" heating or cooling needed to maintain the temperature rate, and it is caused by the extra energy addition or subtraction needed to transform the crystal structure. All first-order phase transformations are associated with latent heat of transformation regardless of the form of the phases. As a familiar example of a phase change, latent heating/cooling is required to cause ice to melt or reform, although that is a solid–liquid transformation. The current case, by contrast, is a solid–solid transformation. The latent heat is smaller, 15–20 J/g, compared to ice water, 334 J/g. Also, the transformation temperature is path dependent, while melting or freezing of water ice at atmospheric pressure occurs at 0°C with little hysteresis. Unlike water-ice, martensitic transformations usually occur under nonequilibrium thermodynamic conditions, thereby exhibiting overall temperature hysteresis, a finite width in the latent heat peaks, and possible rate dependence (discussed later) in the DSC measurements.

The material state, therefore, is quite history dependent, and transformations occur in a multistep manner, as is typical for Ni-rich NiTi alloys (such as ours) that have been heat treated by the supplier. Note in particular that between M_s and A_s, the material state can be either thermal-*R* or thermal-*M* depending on the prior temperature history. The shape memory wire, for example, can exist in either phase at RT as seen in Fig. 3a. Thus, the as-received wire is presumably thermal-*R* since the history involved heat treatment by the supplier at much higher temperatures. During cooling, separate peaks are evident for the sequential $A \rightarrow R$ and $R \rightarrow M$ transformations in Fig. 3a and b. Upon heating, however, the austenite peak has a single large peak in Fig. 3a but has a strange double-hump shape in Fig. 3b. The latter reveals that separate, but overlapping, $M \rightarrow R$ and $R \rightarrow A$ martensitic transformations actually occurred during heating. Often, these two peaks overlap to an extent that they cannot be distinguished, resulting in one large peak (as in Fig. 3a).

The specific latent heat Λ (per unit mass) for a given transformation is obtained by integrating the shaded area of the peak by

$$\Lambda = \int_{t_1}^{t_2} \dot{q}_L(t)\, dt, \qquad (1)$$

where $q \equiv Q/m$ is the heat energy per unit mass, m is the mass of the sample, and t_1 and t_2 are the respective initiation and

ending times of the transformation on the baseline. The specific latent heat power history $\dot{q}_L(t)$ is given as follows:

$$\dot{q}_L(t) = \dot{q}(t) - \dot{q}_C, \tag{2}$$

where $\dot{q}(t)$ is the specific power history measured by the DSC and $\dot{q}_C$ is the specific sensible heat power (associated with the specific heat of the material) estimated along the baseline (nearly a constant for NiTi). Alternatively, the latent heat can be written as follows:

$$\Lambda = \int_{T_1}^{T_2} \frac{dq_L}{dT}\, dT, \tag{3}$$

where $T_1 = T(t_1)$ and $T_2 = T(t_2)$ are the respective initiation and ending temperatures chosen along the baseline, and $dq_L/dT = \dot{q}_L(t)/\dot{T}(t)$, where $\dot{T}$ is the temperature scan rate. We have converted the raw power measured by the DSC to $\dot{q}/|\dot{T}|$in Fig. 3, where $\dot{q}$ is the power per unit mass to make a clear graphical interpretation of the signed shaded areas of the thermogram as latent heats. The remaining area for each heating/cooling direction between the baseline and 0 is associated with the sensible heat changes. Note that T_1 and T_2 should encompass the entire temperature range of the transformation and will be slightly different than the "start" and "finish" temperatures obtained by the dotted construction lines. The latent heats for the $A \rightarrow R$ transformation are about -6.7 and -5 J/g for the respective alloys. The latent heats for the $R \rightarrow M$ transformation are about -6.9 and -6 J/g for the respective alloys, although this one has a larger uncertainty due to the slope and curvature of the baseline cooling curve. The lumped latent heats during $M \rightarrow R \rightarrow A$ transformation during heating are about 19.7 and 15 J/g, respectively. Note that if the specimen had only been cooled to -50°C or so, only one peak would exist on cooling ($A \rightarrow R$), and the peak on heating would have a smaller latent heat since it would only include the $R \rightarrow A$ contribution. Such a thermogram often creates confusion if one does not recognize that the martensite transformation has been cut off. This is a common pitfall when dealing with RT superelastic NiTi where the martensite transformation occurs at very low temperatures, requiring a DSC capable of liquid nitrogen cooling.

Typically, the heating and cooling transformations between A and R exhibit little hysteresis, less than about 2°C. The transformations between A and M, however, are quite hysteretic, exhibiting 80 and 75°C temperature offsets between the heating and the cooling peaks for the respective alloys. Digressing for a moment, we should mention here that both transformations, the "large one" $A \leftrightarrow M$ and the "smaller one" $A \leftrightarrow R$, are technically considered "thermoelastic martensitic transformations" (not to be confused with the names of the phases) in the sense that they are diffusionless and reversible (yet hysteretic). Both have a shape memory effect relative to austenite that can be used in applications, yet the former is better known since it has a larger strain change (≈5%) compared to the latter (≈0.5%). The large hysteresis of the $A \leftrightarrow M$ transformation, however, has an adverse effect on the cyclic stability and ultimate fatigue resistance under transformation cycling. Conversely, the $A \leftrightarrow R$ transformation has better cyclic repeatability, so it might be useful, depending on the intended application, if the smaller strain change and smaller stress level are acceptable. The reason for the dramatic difference in hysteresis between the two transformations is the fact that the rhombohedral R-phase crystal structure is kinematically compatible with that of A, whereas the monoclinic structure of M is not compatible with A, requiring internal twinning of M to produce approximately compatible habit planes between M and A with consequent plasticity near the interface (see Bhattacharya[9] for a more complete discussion of kinematics and compatibility requirements in NiTi crystals). In any event, the large hysteresis between the onsets of transformation (M_s vs. A_s) is generally attributed to nucleation energy barriers, associated with compatibility requirements at the microscale, that must be overcome to initiate transformation. The width of the latent heat peak (e.g., $A_f - A_s$) is due to resistance to growth (frictional kinetics) of the daughter phase within the parent phase. These features arise due to the strong role compatibility plays in the nucleation and kinetics of martensitic phase transformations. By comparison, these energy barriers are more easily surmounted during diffusional phase transformations or liquid–solid phase transformations where thermal activation is dominant (perhaps more familiar to typical metallurgists and thermodynamicists).

As can be seen in Fig. 3, the specific heat of the material is about 0.45–0.50 J/(gK) in the austenite range. The curvature of the baseline seems to be sensitive to the tuning/calibration of the DSC machine, especially at very low temperature where liquid nitrogen cooling is required. Based on our experience, the specific heat in the martensite range seems to be about the same as for austenite. We should point out that many material supplier property tables have reported a value of 0.87 J/(gK) for the specific heat of Nitinol, but we suspect it was incorrectly extracted from the maximum $\dot{q}$ of a latent heat peak, meaning that it included both specific heat and latent heat contributions.

Some Recommendations on DSC Measurements

Specimen preparation can affect the quality of the results. It is important to ensure good thermal contact between the sample pan and the material specimen, which will ensure that the temperature read by the DSC thermocouple accurately measures the temperature of the sample. This is generally optimized by having thin, flat specimens. For wire, we cut it into a number of short lengths and placed them side by side (see Fig. 4), creating a single layer of material that fills the sample pan (to approximate the shape of a wafer). Cutting the wire should be done in a manner to avoid plastic deformation, which introduces residual stresses that would skew the results, so we carefully cut the wire using a diamond cutoff saw. The lid is placed over the sample and crimped to ensure good thermal contact. It is also important to keep the specimen free of contaminants, including moisture, to avoid introducing unwanted artifacts into the thermogram.

Despite the fact that the transformations are generally characterized as *athermal*, meaning that they are neither thermally activated nor rate dependent according to the usual Arrhenius law (which would apply to diffusional transformations), the consistency of the DSC measurements can be

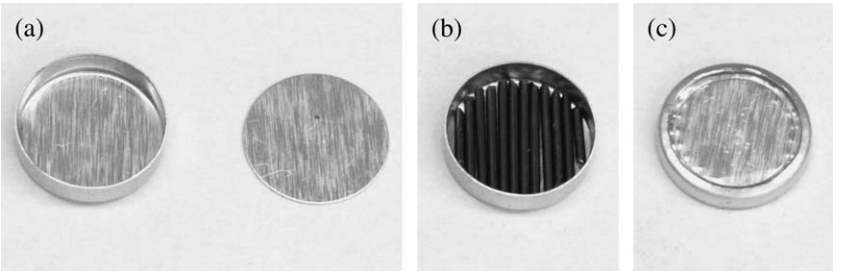

Fig. 4: Photographs of (a) sample pan and lid, (b) wire specimens, and (c) crimped assembly for DSC

affected by the heating/cooling rate specified by the user. Commonly, a rate of ±10°C/min is used (as used in Fig. 3), which is a compromise between trade-offs. Higher rates tend to give sharper enthalpy peaks, which can be integrated more accurately, but may not give accurate transformation temperatures due to thermal lag. Lower temperature rates will reduce thermal lag, but excessively slow rates can make the enthalpy peaks rather indistinct.

BASIC THERMOMECHANICAL BEHAVIOR

Here, we briefly describe the underlying micromechanical mechanisms responsible for the shape memory behavior and superelasticity of SMAs. Two thermomechanical experiments are then presented to demonstrate these features for the two alloys previously addressed.

Shape Memory and Superelasticity

Under stress-free conditions, the low-symmetry martensite lattice can exist in several lattice correspondence variants (12 in the case of Nitinol), which are reflections or rotations of each other. Consequently, martensite can exist in many different microstructures depending on the thermomechanical history (see Bhattacharya[9] for details on the connections between lattice parameters and compatible microstructures). Thermal-martensite is internally twinned, where twin-related variants create a coherent mirror image of the lattice across each twin boundary (special crystallographic planes). Some requirements for shape memory behavior to exist are as follows: (1) the transformation between austenite and martensite occurs with little volume change and (2) the distortional strains relative to austenite are relatively small, typically on the order of 10%. In other words, the structure change can occur by small, coordinated shifts of the atomic positions without diffusion or plasticity. The shape memory effect arises from the fact that martensite can arrange itself into a self-accommodating, finely twinned (heterogeneous) structure with little or no macroscopic strain relative to austenite. Hence, upon cooling from austenite to martensite, little, if any, strain (or shape change) is usually observed (unless the material has been heavily processed to have a so-called two-way shape memory effect). We call this self-accommodated form *thermal-martensite*.

If the martensite becomes sufficiently stressed at cold temperatures, it exchanges certain variants by the motion of twin boundaries to others more preferentially aligned with the stress, which we term *oriented-martensite* or *tensile-martensite*. (Historically, thermal-martensite and tensile-martensite have often been called twinned-martensite and detwinned-martensite, respectively [even by us], but this is a bit misleading since martensite in most SMA polycrystals cannot be completely detwinned to a single variant without concurrent plastic slip.) The resulting macroscopic strain remains upon removal of the stress since all variants are again energetically equivalent. Figure 5 shows transmission electron micrographs, for example, taken by Nishida et al.[10] of equiatomic NiTi specimens in the martensite phase before and after tensile testing taken to several different residual strains after unloading. Thermal-*M* is shown in Fig. 5a before loading with a mixture of many twins in a self-accommodating arrangement. Tensile-*M* is shown in Fig. 5b at 6.4% strain with relatively few twins remaining (and some roughening due to plasticity), while Fig. 5c and d shows further roughening due to plasticity, yet some twins remain even at these extreme strains (which is thought to be partly responsible for the material's excellent ductility by providing an alternate, and reversible, accommodation mechanism to plastic slip). In our case with Ni-rich Nitinol, the aging treatment results in a fine dispersion of Ni_4Ti_3 precipitates that greatly improves resistance to slip compared to equiatomic NiTi,[11] which promotes good superelasticity at high stresses. Upon stress-free heating, the structure reverts back to the cubic austenite and the strain is recovered, provided little plasticity has occurred during loading. The initial shape of the specimen is recovered since the required atomic shifts are relatively small and the high-symmetry cubic structure is unique relative to the martensite variants. This sequence is the mechanism of the shape memory effect.

At high temperatures (above A_f), the material is stable in the austenite phase under stress-free conditions. Adding sufficient stress (isothermally), however, can destabilize austenite in favor of one or more martensite variants (called *stress-induced martensite*, similar in microstructure to tensile-martensite discussed previously but arrived at by a different process) and a macroscopic strain occurs. During subsequent removal of the stress, another lower critical stress is reached at which martensite is no longer thermodynamically stable and the material reverts to austenite, and the strain is recovered upon complete unloading. This isothermal, yet hysteretic (in stress), sequence is the mechanism of superelasticity.

Two Thermomechanical Experiments

Figure 6 shows experimental results (data taken from Shaw[12]) on the shape memory wire in a three-dimensional plot against stress (vertical axis), strain (horizontal axis), and temperature (oblique axis). The stress is measured by P/A_0, axial load over initial cross-sectional area. Strain is measured as δ_e/L_e based on the elongation (δ_e) and gage

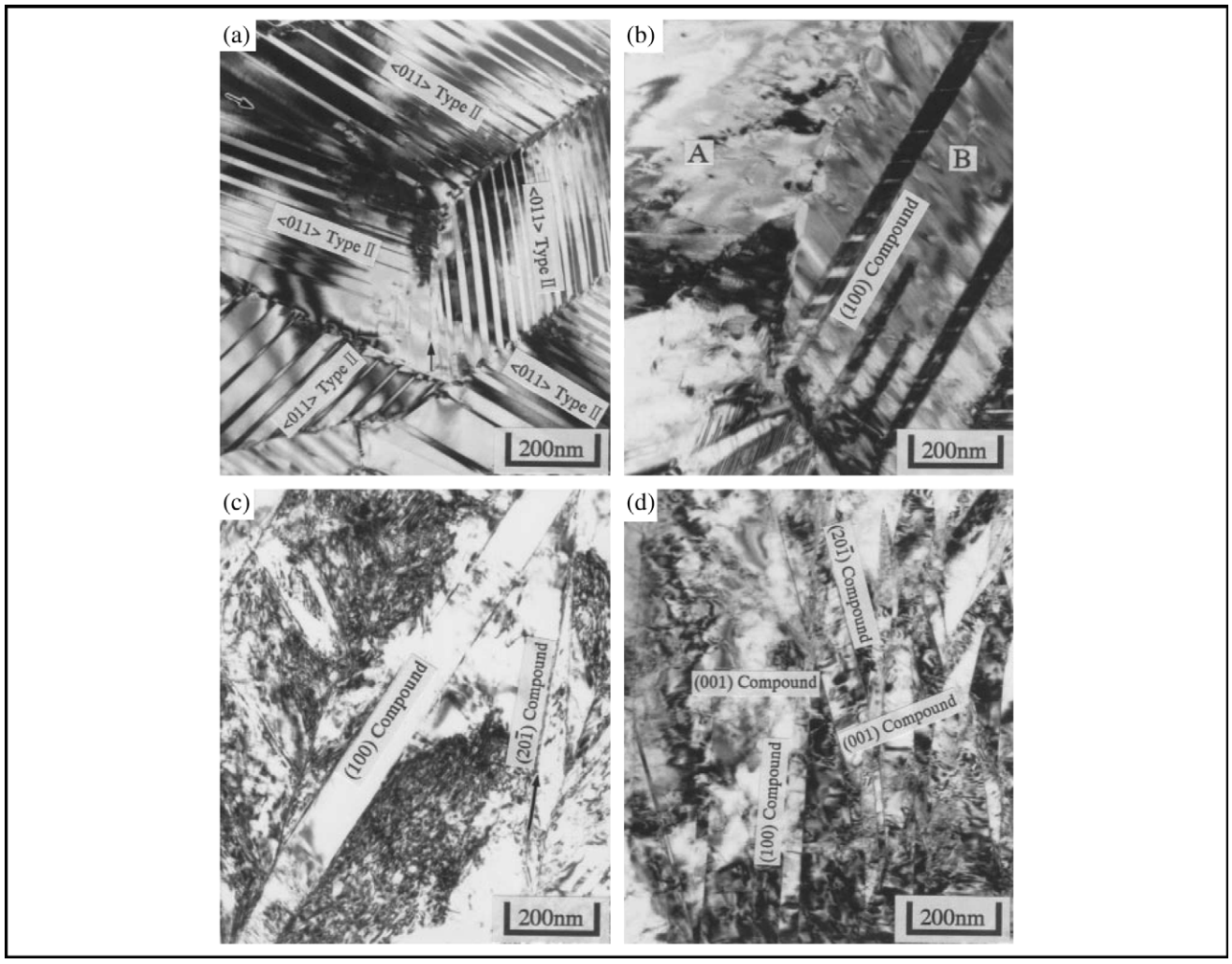

Fig. 5: Transmission electron micrographs of martensite in a NiTi alloy at residual strains: (a) 0%, (b) 6.4%, (c) 11.3%, and (d) 24%. Images taken from Nishida et al.[10] (Reprinted with permission from Elsevier, http://www.sciencedirect.com/science/journal/13596462.)

length (L_e) of a miniature, waterproof extensometer. Temperature (T) is measured by a 76-μm exposed junction K-type thermocouple attached to the specimen. The diameter and free length of the specimen were d = 1.02 mm and L = 63.5 mm, respectively. The specimen had been quenched in liquid nitrogen (77 K) to ensure that it started in the thermal-M phase. The experiment was performed in a conventional electromechanical testing machine (Instron, Norwood, MA) with the specimen immersed in a special water bath to control the temperature. Initially, the specimen was allowed to warm to only 10°C (state ⓪) and then subjected to a slow isothermal displacement–controlled (δ) load–unload cycle (⓪–②). This process converted the material from thermal-martensite (denoted M) to tensile-martensite (denoted M^+), leaving a 5% residual strain. The testing mode was then switched to load control to maintain a small positive stress, just to avoid buckling of the wire, and the temperature was raised to 70°C while monitoring the strain. The strain was relatively static until the temperature reached above 45°C, at which point the strain decreased rapidly toward 0 (③–④) while the material transformed from tensile-martensite (M^+) to austenite (A) and then it remained static at a small value until state ⑤. This sequence ⓪–⑤ in the experiment demonstrates quantitatively the shape memory effect.

Next, an isothermal load–unload cycle was imposed under displacement control again at 70°C (⑤–⑩ in the figure), which demonstrates superelasticity in the same specimen. Between states ⑤ and ⑥, the austenite response is nearly linearly elastic, like a conventional metal, but at ⑥, the apparent tangent modulus suddenly switched to near 0 with elongation continuing at constant stress. The crosshead motion was reversed at ⑦ where the strain was a bit larger than 6%, at which point a large fraction of the specimen was M^+. Unloading proceeded from ⑦ to ⑧ along a nonlinear path with a lower tangent modulus than previously for A (from ⑤ to ⑥). At ⑧, the stress reached another plateau, along which the material reverted to A. This occurs since M^+ (stress-induced martensite) is not thermodynamically stable at this elevated temperature without sufficient stress. Between ⑧ and ⑨, the strain decreased at constant stress until the path nearly met the initial elastic response of A at ⑨. The final segment between ⑨ and ⑩ was elastic unloading of A, and the strain was very nearly recovered. Note that the recovery of strain occurred

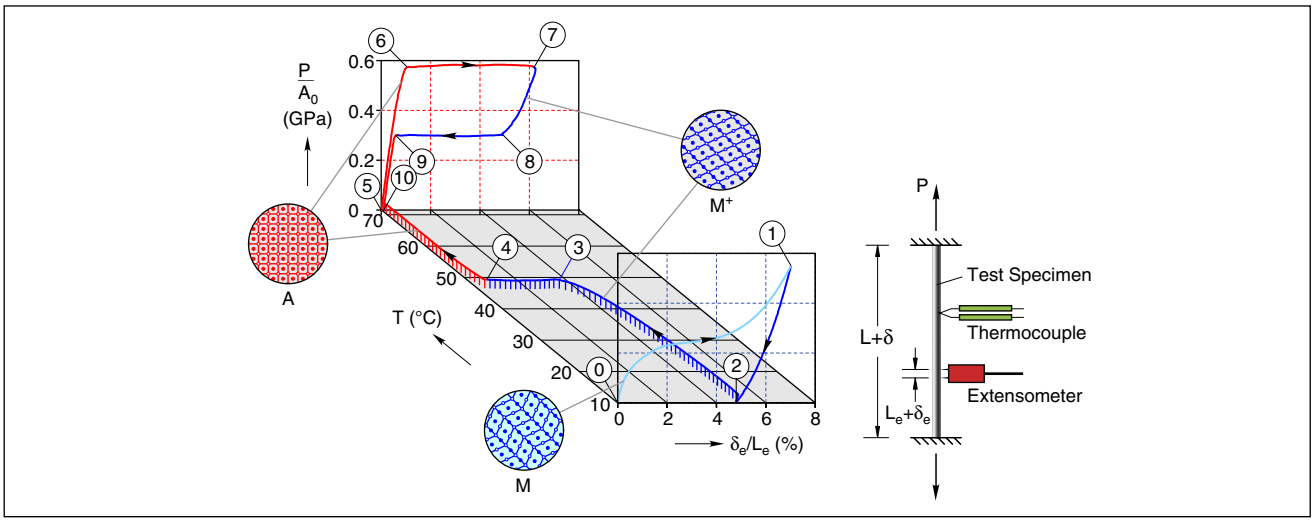

Fig. 6: Thermomechanical experiment on shape memory Nitinol: shape memory effect (⓪–⑤) and superelasticity (⑤–⑩). Data taken from Shaw[12]

through a large hysteresis, indicating that a significant portion of work energy was dissipated in the material during this cycle. (In this regard, "superelasticity" is a bit of a misnomer since while the strain is in fact recovered, the process is not "elastic" in the sense normally used in mechanics [which requires path independence during loading and unloading]. Accordingly, some prefer to call this response "pseudoelasticity.")

One should note that in Fig. 6, martensite reorientation (⓪–①) is associated with a relatively soft and nonlinear response, and unloading exhibits a large hysteresis. The initial response of austenite in Fig. 6 (⑤–⑥) is stiff by comparison. (Incidentally, this is opposite to the well-known case of carbon steel, where austenite is the soft phase and martensite is the hard phase. The austenite in steel has a cubic structure and martensite has a tetragonal structure. A shape memory effect is not possible in steel since the transformation involves a significant volume change, requiring a large energy barrier to be surmounted.) The overall thermomechanical response is quite nonlinear and involves significant hysteresis, or path dependence, in stress–strain–temperature, so it is impossible to develop a simple function that relates stress, strain, and temperature in an algebraic way. Consequently, many constitutive models have been proposed that only treat certain aspects of the behavior or are developed according to time-dependent formulations, making it a challenging and ongoing research topic still today.

Figure 7 shows the results of a similar experiment performed on superelastic wire. Qualitatively, the features described above are the same, except that the transformation temperature is lower so that the material is superelastic at RT, and the shape memory effect is observed by chilling the material to subambient temperatures, then loading/unloading, and then allowing it to warm to RT. For this alloy, the stress required to orient martensite (⓪ and ①) is less than for the shape memory wire. This experiment was performed in a temperature-controlled air chamber rather than in a water bath due to the low temperatures involved. As a result, the temperature control is not as precise and the path between ③ and ④, during the shape memory recovery, is somewhat jagged compared to the previous case in water. The strain measurement was obtained by a laser extensometer system (model EIR-05; Electronic Instrument Research, Irwin, PA) exterior to the chamber that transmitted a planar laser sheet through the viewing glass of the chamber and received a signal reflected from retroreflective tags attached to the wire specimen. (Similar material is used as reflective decals on athletic shoes.)

SUMMARY AND CONCLUSIONS

Our intent in this series of articles is to provide recommendations for characterizing Nitinol SMA wire. We wish to forewarn experimentalists, who are relatively inexperienced with SMAs, of some pitfalls regarding experimental technique and interpretation of the data.

This article provided DSC thermograms of the two Nitinol wire alloys, one that is austenite (stress free) above RT (shape memory wire) and one that is austenite at RT (superelastic wire), as a first step to characterize the materials. These were used to measure the transformation temperatures in the material, including start and finish temperatures for three martensitic transformations: $A \rightarrow R$ (R_s and R_f on cooling), $R \rightarrow M$ (M_s and M_f on cooling), and $M \rightarrow A$ (A_s and A_f on heating). Furthermore, we showed how to extract specific latent heats of transformation and the specific heat of the material, providing recommendations for obtaining accurate data. The measured specific heat for both alloys was approximately the same, near 0.45 J/(gK), yet the latent heats of transformation were quantitatively different, 19.7 versus 15 J/g ($M \rightarrow R \rightarrow A$) for the shape memory wire and superelastic wire, respectively. The implications of this difference will be explored further in later articles in this series. In both alloys, the $A \leftrightarrow M$ hysteresis was approximately 75–80°C, and this is an important parameter to measure for each alloy used to quantify the

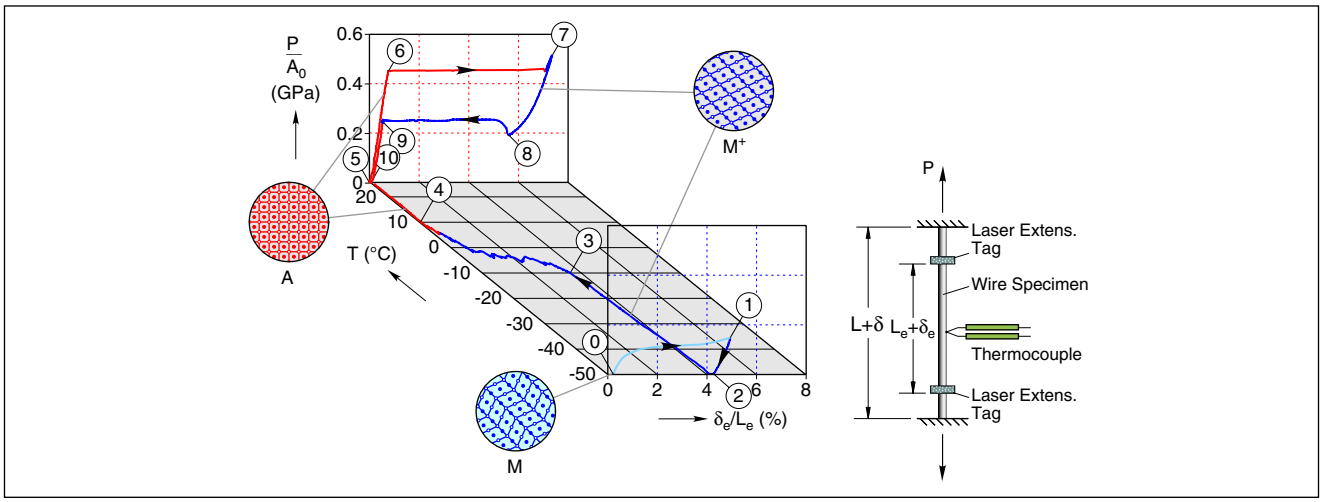

Fig. 7: Thermomechanical experiment on superelastic Nitinol: shape memory effect (⓪–⑤) and superelasticity (⑤–⑩). Data taken from Chang et al.[8]

inherent hysteresis in the material. We then described the phenomena of shape memory and superelasticity and the underlying microstructural mechanisms of the martensitic transformations responsible for both. Thermomechanical data were presented on the two Nitinol wires. Both exhibited shape memory and superelasticity but in different temperature regimes.

The next article in the series (part 2) will address isothermal mechanical experiments over a wide range of temperatures for the same two Nitinol wire alloys and will map the various material phases in stress–temperature space. Experimental techniques will be discussed in order to achieve a consistent, high-quality data set of the fundamental temperature sensitivities involved.

ACKNOWLEDGMENTS

Our thanks go to Nilesh Mankame (General Motors) for the invitation to write this series of articles. The experimental techniques developed and experience gained to write this series of articles were the results of many years of work by Shaw and graduate students at the University of Michigan as well as Shaw's graduate work at the University of Texas at Austin under the guidance of Stelios Kyriakides. Several prior University of Michigan graduate students, including Bi-chiau Chang, Antoine Gremillet, Brian MacLachlan, and Geoffroy Lenglin, have contributed to development of the experimental techniques described here and in forthcoming articles in this series. Helpful comments on this article from Ben Reedlunn are acknowledged with thanks. The authors wish to sincerely thank the National Science Foundation for their continuing financial support. The authors (Shaw and Churchill) also wish to express their gratitude to General Motors Corp. for their financial assistance and ongoing collaboration through the General Motors/University of Michigan Collaborative Research Laboratory in Smart Materials and Structures.

References

1. Duerig, T.W., Melton, K.N., Stöckel, D., and Wayman, C.M. (eds), *Engineering Aspects of Shape Memory Alloys*, Butterworth-Heinemann, Boston, MA (1990).

2. Otsuka, K., and Wayman, C.M. (eds), *Shape Memory Materials*, Cambridge University Press, Cambridge, UK (1998).

3. Schwartz, M., *Encyclopedia of Smart Materials*, Volume 1, John Wiley and Sons, New York, NY (2002).

4. Otsuka, K., and Ren, X., "Physical Metallurgy of Ti-Ni-Based Shape Memory Alloys," *Progress in Materials Science* **50**:511–678 (2005).

5. Brei, D., Luntz, J., Shaw, J.A., et al. "General Motors and the University of Michigan Smart Materials and Structures Collaborative Research Laboratory," *Proceedings of the SPIE 14th Annual International Symposium on Smart Structures and Materials*, March 8–22, 2007, San Diego, CA (2007).

6. Callister, W.D., Jr, *Materials Science and Engineering: an Introduction*, 6th Edition, John Wiley and Sons, New York, NY (2003).

7. Shaw, J.A., and Kyriakides, S., "Thermomechanical Aspects of NiTi," *Journal of the Mechanics and Physics of Solids* **43**(8):1243–1281 (1995).

8. Chang, B.C., Shaw, J.A., and Iadicola, M.A., "Thermodynamics of Shape Memory Alloy Wire: modeling, Experiments, and Application," *Continuum Mechanics and Thermodynamics* **18**(1–2): 83–118 (2006).

9. Bhattacharya, K., *Microstructure of Martensite: why It Forms and How It Gives Rise to the Shape-Memory Effect. Oxford Series on Materials Modelling*, 1st Edition, Oxford University Press, New York, NY (2003).

10. Nishida, M., Ii, S., Kitamura, K., et al. "New Deformation Twinning Mode of B19' Martensite in Ti-Ni Shape Memory Alloy," *Scripta Materialia* **39**(12):1749–1754 (1998).

11. Frick, C.P., Ortega, A.M., Tyber, J., et al. "Thermal Processing of Polycrystalline NiTi Shape Memory Alloys," *Materials Science and Engineering: A* **405**(1–2):34–49 (2005).

12. Shaw, J.A., *Material Instabilities in a Nickel-Titanium Shape Memory Alloy*, PhD Dissertation, The University of Texas at Austin, Department of Aerospace Engineering, Austin, TX (1997). ■